ADVANCED FUNCTIONAL MATERIALS
www.afm-journal.de

Polymer Microparticles with Controllable Surface Textures Generated through Interfacial Instabilities of Emulsion Droplets

*Shanqin Liu, Renhua Deng, Weikun Li, and Jintao Zhu**

A general and versatile route to prepare hierarchical polymer microparticles via interfacial instabilities of emulsion droplets is demonstrated. Uniform emulsion droplets containing hydrophobic polymers and n-hexadecanol (HD) are generated through microfluidic devices. When organic solvent diffuses through the aqueous phase and evaporates, shrinking emulsion droplets containing HD and polystyrene (PS) will trigger interfacial instabilities to form microparticles with wrinkled surfaces. Interestingly, surface-textures of the particles can be accurately tailored from smooth to high textures by varying the HD concentration and/or the rate of solvent evaporation. Moreover, composite particles can be generated by suspending different hydrophobic species to the initial polymer solutions. This versatile approach for preparing particles with highly textured surfaces can be extended to other type of hydrophobic polymers which will find potential applications in the fields of drug delivery, tissue engineering, catalysis, coating, and device fabrication.

1. Introduction

Polymer particles with different compositions and morphologies have received increasing attentions since their properties (such as optical, electrical, and chemical) can be tuned with the structure, size, and composition, making them ubiquitous for various applications in biotechnology, pharmacology, chemical industry, and so forth.[1–4] Recently, more and more interest has been focused on anisotropic particles, which are anisotropic in shape and/or surface chemistry. Particles topographies can significantly affect their chemical and physical properties, e.g., catalytic performance and efficiency, assembly structures, platelet adhesion, biodistribution, and bioresponse.[5–7] For instance, particle surface-morphology influences the assembly structures through their mutual interactions when the particles are used as new types of building blocks for self-assembly. More interestingly, surface roughness plays a crucial role in regulating the interactions between biomaterials and biological systems—rough surface will be of benefit in cell adhesion, spread, and growth, and tissue healing due to its structural resemblances to extracellular networks. Inspired by this concept, manipulating surface microstructure offers a new opportunity of designing new biomaterials to tailor cell functions, such as stem cell differentiation for tissue engineering in vitro and in vivo.[8,9]

In general, polymer particles prepared by polymerization in heterogeneous systems (e.g., emulsion, suspension, and dispersion polymerization, etc.) have a spherical shape due to the minimization of interfacial free energy between the particle and the medium.[10–12] Several attempts have been established, including lithography,[1] modified seeded-emulsion-polymerization,[13] suspension polymerization,[14] and interfacial instabilities of emulsion droplets containing amphiphilic block copolymers,[15–18] to generate microparticles with convoluted surfaces. Yet, it still remains a challenge to produce polymer particles with controllable surface roughness for a variety of applications.

Here, we demonstrate a facile, yet robust strategy to prepare polymer microparticles with controllable surface-textures by interfacial instabilities of emulsion droplets containing *hydrophobic polymers* and n-hexadecanol (HD) which acts as a cosurfactant. Using our strategy, the size/surface topography of microparticles can be readily tailored by adjusting HD concentration (C_{HD}) and/or the rate of solvent evaporation. This approach can be applied to different polymers and allows us to functionalize the polymer particles with tailored chemical/physical properties by incorporating functional species. These particles may find applications in coating, catalysis, and drug delivery.

2. Results and Discussion

2.1. Convoluted Microparticles Generated through Interfacial Instabilities

Our experimental method is illustrated in **Figure 1**. Monodisperse emulsion droplets with tunable size of 30–70 μm were generated through a microcapillary device by varying the exit orifice size and/or flow rates of the two phases.[12,15] As

S. Q. Liu, R. H. Deng, W. K. Li, Prof. J. T. Zhu
Hubei Key Lab of Materials Chemistry
and Service Failure School of Chemistry
and Chemical Engineering
Huazhong University of Science and Technology
Wuhan, 430074, P. R. China
Fax: (+86) 27875-43632
E-mail: jtzhu@mail.hust.edu.cn

DOI: 10.1002/adfm.201103018

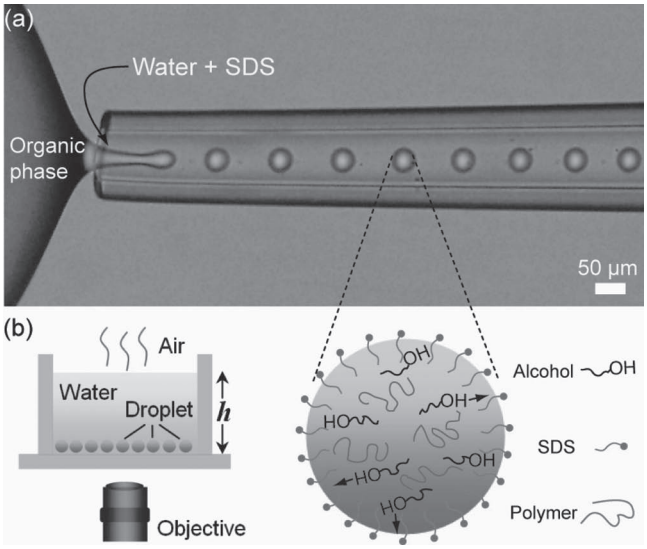

Figure 1. a) Optical microscopy image showing emulsion droplets formation in a microcapillary device. The organic phase consists of polystyrene (PS) and HD in chloroform, and aqueous phase consists of 3 mg/mL sodium dodecyl sulfate (SDS) stabilizing the emulsion droplets against coalescence; b) Schematic illustration displays experimental setup for adjusting solvent evaporation rate by varying height of water layer (*h*).

displayed in Figure 1a, the organic phase flow passes through the exit orifice and subsequently ruptures to form uniform emulsion droplets just inside the orifice as a result of interfacial tension. After generation, the emulsions were collected into a small cell and chloroform was allowed to remove by diffusing through the aqueous layer and evaporate into the surrounding air at ambient temperature (25 °C). The rate of solvent evaporation is controlled by tailoring height of the water layer (*h*) which regulates the diffusion distance of chloroform solvent (Figure 1b). Depending on *h*, evaporation process of the emulsion droplets will last tens of minutes to hours.

Upon solvent removal, decrease in the area of the interface of the shrinking droplets causes a non-equilibrium adsorbed interfacial excess of both SDS and HD, triggering an interfacial instability—the droplets underwent "explosion" or instability by which their interfacial areas spontaneously increased (see the Supporting Information (SI) Movie S1 and S2). The chloroform/water interface became highly corrugated (**Figure 2**b) and many wrinkles of microsized fluid extruded out from the droplets (Figure 2c and 2d). Similar interfacial roughening and spontaneously droplet ejection have been found in oil-water-

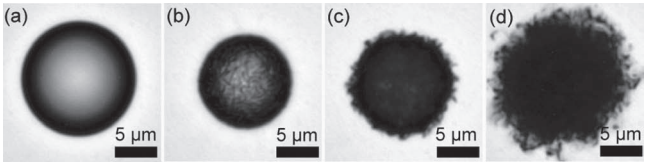

Figure 2. Optical microscopy images showing evolution of the same emulsion droplet containing 10 mg/mL PS_{21k} and 1 mg/mL HD during solvent removal at $h = 0.5$ mm. The time elapse for the images was: a) 0 s, b) 49 s, c) 51 s, and d) 66 s.

amphiphiles, polymer blends, and emulsion droplets containing amphiphilic block copolymers.[15,19–24] Adsorption of surfactant to the oil/water interface or excess segregation of block copolymers to the interface of polymer blends will significantly decrease the interfacial tension. As interfacial excess increase, the interfacial tension is predicted to decrease to zero or transiently negative value, at which point the interface becomes unstable, triggering the ejection of tiny droplets or interfacial roughening. Theoretically, Granek and collaborators reported a model for spontaneous emulsification for oil-water-surfactant ternary system resulting from a transiently negative interfacial tension of water/oil, which was achieved by strong adsorption of surfactant to the interface.[22] Moreover, Hu and coworker pointed out that the preferred interfacial curvature of the amphiphiles could induce interfacial instability even at slightly positive value of interfacial tension.[25] In the previous reports, Zhu and Hayward reported similar but qualitatively different interfacial instabilities of emulsion droplets containing amphiphilic block copolymers PS-*b*-poly(ethylene oxide) (PS-*b*-PEO), where fluid tendrils or tiny emulsion droplets will grow at the interfaces.[15,18,26] Correlation of the approach of interfacial tension to zero leading to the interfacial instabilities has been experimentally evidenced for polymer blends systems and emulsion droplets containing amphiphilic block copolymers.[16,20,21,27,28]

In this paper, we introduce a new and versatile way to induce the vanishing of interfacial tension and interfacial instabilities by adding cosurfactant HD to the emulsion droplets containing *hydrophobic* polymers stabilized by SDS. It is worth noting that HD is a widely used cosurfactant which can reduce the interfacial tension of oil/water further besides the added surfactant, ultimately leading to the spontaneous emulsification of hydrocarbon/surfactant/alcohol ternary system.[19] The vanishing of the interfacial tension for such system can be understood from the Gibbs adsorption equation relating interfacial free energy to the amphiphiles excess (Equation 1):[24]

$$d\gamma = \sum_i v_i \mu_i \tag{1}$$

Where γ is the interfacial free energy, v_i is the interfacial excess of component i in molecules per unit area and μ_i is the chemical potential of component i on a per molecule basis. Clearly, the reduction of the interfacial tension of the oil/water depends on the contributions from the surfactant (e.g., SDS) and HD. Specifically, SDS will decrease the interfacial tension of the emulsion droplets to low value while HD produces its own contribution to the decrease of the interfacial tension to extremely low or even transiently negative value.

Thus, in this work, we presume that interfacial tension will markedly decrease or even vanish upon the removal of solvent due to the increase of the concentration of dissolved HD,[29] which plays key roles in the interfacial instability: i) HD molecules will accumulate and interpenetrate to the SDS monolayer at organic/water interface, leading to the reduction of interfacial tension; ii) Migration of HD molecules to the organic/water interface will induce the rearrangement of SDS molecules at the interface, further inducing SDS assemblies curvature modification and the reduction of the interfacial tension.[30] The vanished interfacial tension will drive interfacial roughening

of the shrinking droplets. The organic/water interfacial area will spontaneously increase by folding or deforming of the interface instead of ejecting tiny droplets due to the increased bulk viscosity of the droplet.[18,19] The whole process will last ~1 min, and the wrinkles on the particles are then frozen due to high viscosity of the fluid and the glassy nature of PS after complete solvent removal. Final products of the interfacial instabilities are the highly textured particles which have a spherical profile (overall diameter: ~15 μm, see Figure 2, Figure S1 and S2), but with a highly-roughened surface, consisting of many irregular protrusions (size: ~ 70 nm–5 μm, depending on the processing conditions).

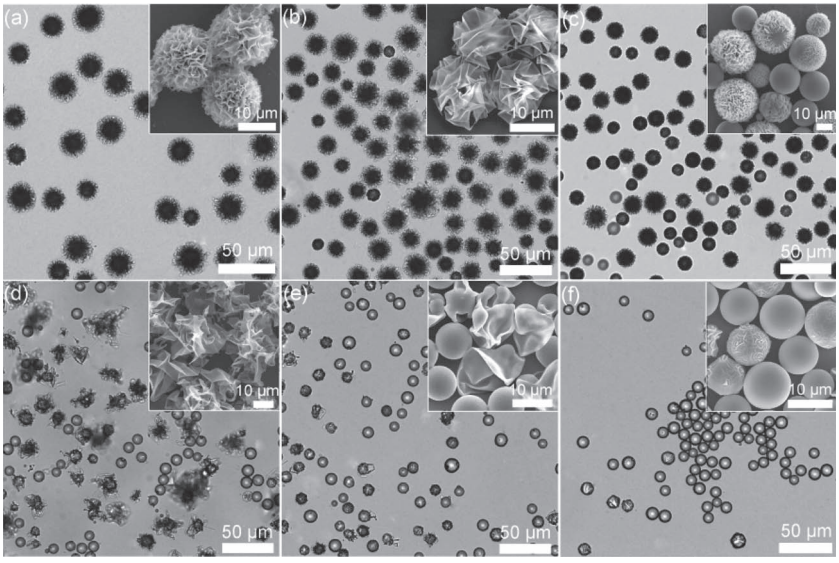

Figure 4. a–f) Optical microscopy images of the microparticles with different surface-roughness which were obtained from emulsion droplets containing 10 mg/mL PS_{21k} and 1 mg/mL HD with varied water layer height: a) h = 0.5 mm, b) h = 2 mm, c) h = 3 mm, d) h = 5 mm, e) h = 7.5 mm, f) h = 10 mm. 3 mg/mL SDS was added to the aqueous phase to stabilize the emulsion droplets. Insets in the upper right are the representative SEM images.

2.2. Microparticles with Tailored Surface-Textures

The degree of wrinkles (e.g., protrusion length) on the particles can be tuned by simply adjusting C_{HD} and/or the rate of solvent evaporation. Monodisperse particles with smooth surfaces were obtained when initial C_{HD} was lower than 0.1 mg/mL (**Figure 3**a). As increasing C_{HD} from 0.3 to 3 mg/mL, surface features increased gradually from slight to enhanced wrinkles (Figure 3b–f). All of the different products described above showed a quite narrow size distribution and rich morphologies. Brunauer–Emmett–Teller (BET) result shows that specific surface area for the smooth (Figure 3a) and roughened particles (Figure 3d) is 2.0 and 19.7 m^2/g, respectively, indicating that particles with rough surface have a high surface-to-volume ratio. When C_{HD} was above 5 mg/mL, qualitatively different interfacial instabilities were observed and the droplets broke up into tiny droplets and rearranged into sheet-like structures. This phenomenon is beyond the scope of this report and will be presented in a separate paper.

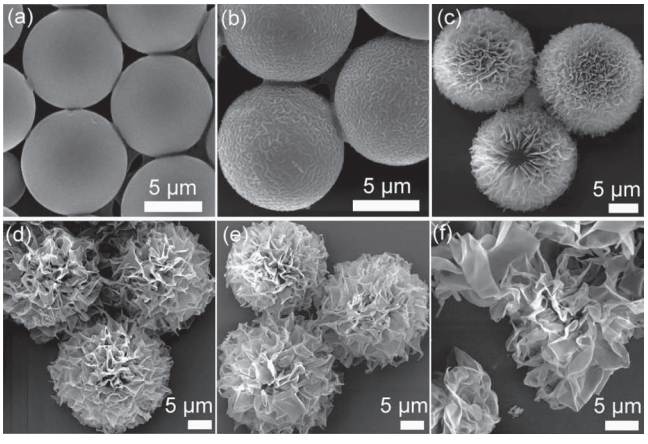

Figure 3. Scanning Electron Microscopy (SEM) images of the microparticles produced from emulsion droplets containing 10 mg/mL PS_{21k} and varied C_{HD}: a) 0 mg/mL, b) 0.3 mg/mL, c) 0.5 mg/mL, d) 0.7 mg/mL, e) 1 mg/mL, f) 3 mg/mL. 3 mg/mL SDS was added to the aqueous phase while h was 0.5 mm.

In addition, solvent evaporation rate plays a crucial role in the interfacial behavior and the final structures. Slow evaporation rate (~10^{-9} μL/s for a single droplet with initial size of ~40 μm, h = 7.5 mm) will suppress the interfacial instability, and microparticles with relatively smooth surfaces are generated (**Figure 4**e and Figure 4f, and Figure S3). However, fast evaporation rate (~ 10^{-6} μL/s for initial droplet size of ~ 40 μm, h = 0.25 mm) will trigger the interfacial instability and form more stable wrinkled microstructures (Figure 4a–d). Thus, surface roughness of the particles can be tuned by simply varying the h besides the variation of C_{HD}. The above results indicated that the critical C_{HD} for the interfacial instabilities varied by tuning the evaporation rate—higher evaporation rate will shift critical C_{HD} to a lower value triggering interfacial instabilities of the droplets. The reason behind this can be understood from the competition between the diffusion rate of HD molecules and the shrinking speed of the droplet. Specifically, distribution of HD molecules in each droplet is generally uniform at the initial stage. Yet, at high evaporation rate, especially when the shrinking speed becomes comparable or great than the HD diffusion rate, accumulated HD molecules near the interfaces do not gain enough time to diffuse back to the bulk droplet and recover the uniform distribution. Obviously, the adsorption and desorption kinetics of the HD from the emulsion droplet interface plays the most important role in the interfacial instabilities. After all the concentration gradient of chloroform in the droplet is toward the droplet interface, diffusion of HD back into the droplet is unlikely to be controlling. In this case, the droplet may thus develop a higher polymer concentration at the aqueous interface, and the increased near-surface concentration will trigger the interfacial instabilities at a lower average HD concentration.

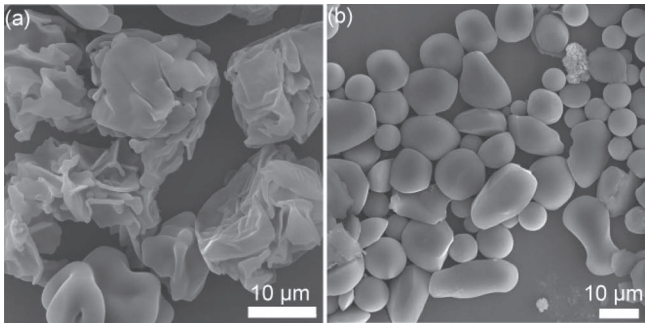

Figure 5. SEM images of the microparticles formed from emulsion droplets containing 1 mg/mL HD and 10 mg/mL PS with different molecular weight of a) $PS_{2.8k}$ and b) PS_{876k}. *h* was 0.75 mm while 3 mg/mL SDS was added to the aqueous phase to stabilize the emulsion droplets.

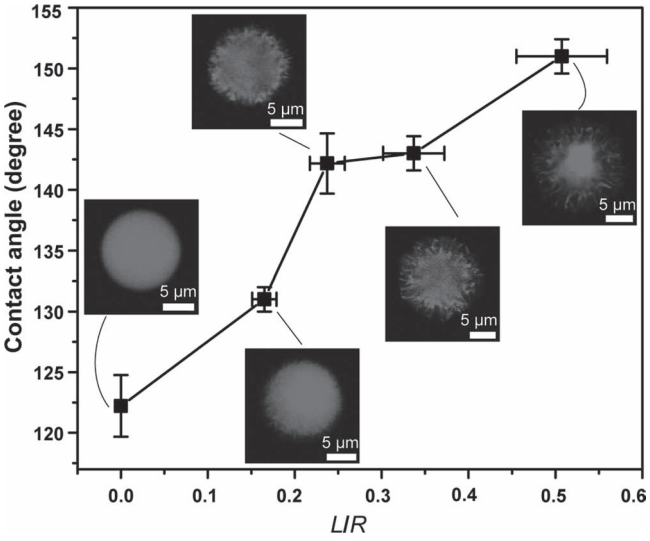

Figure 6. Plot shows relationship between water contact angle with the particles films and the relative protrusion length (*L*/*R*) on the PS_{21k} microparticles, obtained from the measurement of confocal laser scanning microscopy (CLSM) images (see Figure S8 in the SI). *L* and *R* represent protrusion length and radius of overall particles, respectively. Representative CLSM images are shown for the data points. Error bars represent the standard deviation.

Moreover, polymer molecular weight, solvent nature and chain length of the cosurfactant are also important for the interfacial instability and particles structures (see **Figure 5** and Figure S4–S6). For example, emulsion droplets containing $PS_{2.8k}$ would give rise to wrinkles faster than that of PS_{21k} at the same experimental condition. Yet, the highly-textured microstructures could not be fully trapped during solvent removal due to the low viscosity of $PS_{2.8k}$, leading to the microparticles with slight wrinkles on the particles surfaces, as displayed in Figure 5a. However, interfacial instabilities were highly suppressed when PS_{876k} was employed due to the increased viscosity and entanglement of the polymer with high molecular weight.[31] Irregular microparticles with smooth surfaces were obtained when PS_{876k} was employed, as shown in Figure 5b.

More interestingly, we show that these wrinkled particles can be used to prepare superhydrophobic coatings.[32,33] To avoid the influence of the SDS and HD on value of the water contact angle, the particles were dialyzed against water and ethanol to completely remove the SDS and HD before the particles films preparation. As displayed in **Figure 6** and Figure S7 in the SI, our results indicated that water contact angle performed on the particles films increased nearly linearly with the increase of the protrusions on the particles. We conclude that the increase of the contact angle can be ascribed to the contribution of roughness (dual-scale roughness from the protrusion and the particles) and the capability of trapping air among the protrusions to the wettability of the particles films.[33] Remarkably, films of the particles with relative protrusion length of 0.5 (μm) featured water-repellent superhydrophobicity (contact angle: 151.4°, Figure 6).

2.3 Generality of the Approach

To further illustrate the generality of our approach, investigations were performed by replacing PS with several different polymers, e.g., poly (methyl methacrylate) ($PMMA_{24k}$), poly-DL-lactic acid (PLA_{50k}), polybutadiene ($PB_{21.7k}$), and hydrophobic block copolymers, such as PS_{25k}-*b*-$PMMA_{26k}$ (see Figure S9 and S10). Similar interfacial instabilities were observed when these polymers were used. For example, hierarchically dendritic PS-*b*-PMMA microparticles were obtained, as displayed in **Figure 7**a–c.

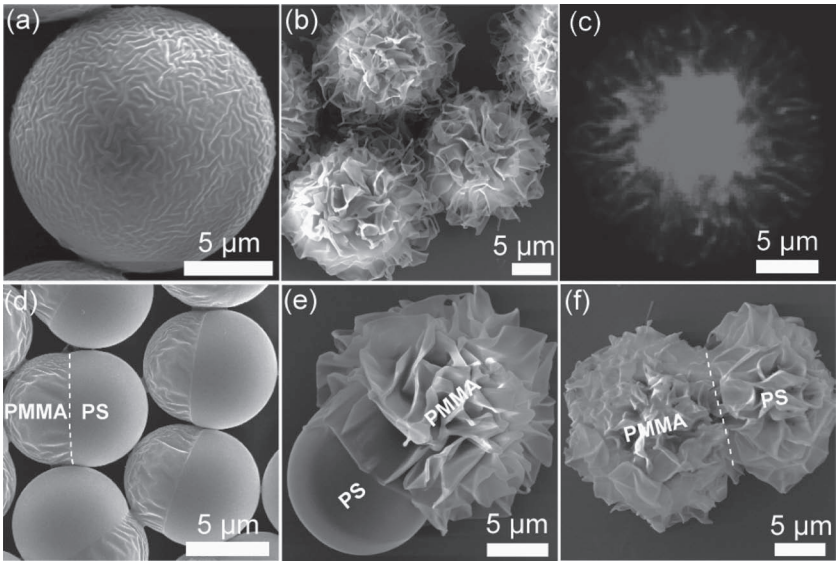

Figure 7. a, b) SEM and c) CLSM images of wrinkled microparticles from emulsion droplets containing 10 mg/mL PS_{25k}- *b* -$PMMA_{26k}$ and varied C_{HD}: a) 0.3 mg/mL HD, b) 2 mg/mL HD, c) 2 mg/mL HD and 0.1 wt% Nile Red relative to the polymer. d–f) SEM images of Janus particles from emulsion droplets containing 10 mg/mL mixtures of PS_{21k} and $PMMA_{24k}$ with weight ratio of 1:1 and varied HD concentration: d) 0.1 mg/mL, e) 0.5 mg/mL, f) 0.7 mg/mL. 3 mg/mL SDS was added to the aqueous phase while *h* was 0.5 mm.

Similarly, the surface roughness of the particles can also be tuned by manipulating experimental parameters as employed in PS system (see Figure S10).

This technique can also allow us to fabricate composite particles to meet the needs of different applications by adding functional species to the initial organic phase. PS/PMMA Janus particles with tunable surface morphologies and patchy ratios can be formed by varying the composition of the immiscible polymer blends and C_{HD}, as shown in Figure 7d–f and Figure S11. Interestingly, Janus particles with controlled roughness in one or both sides can also be generated (see Figure 7d–f). In addition, by suspending small amount of fluorescent dye (e.g., Nile Red) or hydrophobic quantum dots CdSe to the initial dispersed phase, fluorescent dendritic PS-*b*-PMMA microparticles can be generated, as shown in Figure 7c and Figure S8. The uniform fluorescence across the particles suggests that the fluorescent dye or the CdSe nanoparticles are well dispersed in the polymer matrix of the micropartices. Similarly, by suspending hydrophobic magnetic nanoparticles in the initial polymer solution, magnetic dendritic particles are fabricated, as shown in the SI, Figure S12. Moreover, multifunctional polymer microparticles can be generated by dispersing different functional species. The successful incorporation of different functional species into the polymer particles highlights the versatility and robustness of this approach.

3. Conclusions

In summary, we present a general and versatile approach to generate polymer microparticles with controllable surface textures. Interfacial instabilities of emulsion droplets, owning to the reduction of interfacial tension induced by HD, were observed and roughness on the particles surface can be tuned by varying C_{HD}, solvent evaporation rate, and polymer compositions. It is possible to extend this versatile approach to generate convoluted microparticles for a broad range of hydrophobic polymers (see Figure S9 and S10); and the highly uniform dendritic particles can be potentially useful in drug carrier system, catalysis, coating, cosmetics, and tissue engineering.

4. Experimental Section

Materials: $PS_{2.8k}$ (PDI = 1.09), PS_{21k} (PDI = 1.04), PS_{876k} (PDI = 1.19), $PMMA_{24k}$ (PDI = 1.25), PS_{25k}-*b*-$PMMA_{26k}$ (PDI = 1.06), $PB_{21.7k}$ (PDI = 1.05), and PLA_{50k} (PDI = 1.20) were purchased from Polymer Source. Nile Red (purity: 98%) and SDS (purity: 98%) were purchased from Sigma-Aldrich. n-hexadecanol (HD) and other medium chain alcohols were obtained from Shanghai Reagents Co., China. All of the materials were used without further purification.

Sample Preparation: To produce emulsion droplets with well-controlled sizes, we constructed microfluidic devices which consisted of a cylindrical collection tube nested inside a square glass capillary. The tip of the collection tube was tapered to an orifice of ~20–100 μm by using Narishige PC-10 micropipette puller and Narishige MF-900 microforge. The continuous aqueous phase consisted of 30 vol% glycerol, and 3 mg/mL SDS while the dispersed organic phase was 10 mg/mL polymers and HD with varied concentration in chloroform. After generation, the emulsions were collected into a designed round cell with an inner diameter of 2.2 cm, containing ~10 fold excess of 3 mg/mL SDS aqueous solution. The resulting suspension of polymer microparticles was first dialyzed against deionized water for 7 days to remove glycerol, SDS, and residual chloroform, and then dialyzed against ethanol for 7 days to remove HD.

Oleic-acid capped CdSe nanoparticles were prepared by the method described in the literature and grown to a diameter of ~ 4 nm.[34] Oleic-acid coated magnetic nanoparticles (Fe_3O_4, size: ~8 nm) were prepared according to the reported procedure.[35] To prepare nanoparticle-decorated microparticles, nanoparticles (CdSe or Fe_3O_4) at concentration of 0.1 wt% relative to the polymer were suspended in the initial polymer solution. Functional microparticles were then generated through similar way, as described above.

Optical Microscopy: Real-time structural evolution of the shrinking emulsion droplets containing PS and HD was monitored using Olympus IX71 inverted optical microscope in bright-field or fluorescence modes.

Confocal Laser Scanning Microscopy: Particles suspension was examined with a Fluoview FV1000 CLSM equipped with a 1 mW helium–neon laser. Red fluorescence signal, originated from Nile Red, was observed with a long-pass 590 nm emission filter under 515 nm laser illumination. The pinhole diameter was set at 71 mm. Stacks of images were collected every 1 μm along the z-axis.

Scanning Electron Microscopy: The resulting particles morphologies were observed by SEM which was carried out on a Sirion 200 SEM at an accelerating voltage of 10 kV. To prepare samples for SEM, a drop of the dialyzed particles dispersion was dropped on a clean silicon wafer, and water was allowed to evaporate. Then, the samples were coated with a thin layer of gold.

Contact Angle Measurement: The static contact angle of one water droplet (~7 μL) on the particles-film surface was measured on a JC2000C1 contact angle measuring system (Shanghai Zhongchen Digital Technol. Instrument Ltd Co., China) at room temperature (25 °C) with humidity of 12%. To prepare the samples, concentrated microparticles suspensions were deposited on clean silicon wafer, and water was allowed to evaporate under ambient temperature, yielding particles films. Before analysis, the particles films were dried at 50 °C for 12 h under vacuum.

BET Measurement: BET specific surface area, N_2 adsorption isotherms (77.2 K), and pore size distributions of the microparticles were measured by the BET method using a Micrometrics ASAP 2020 M surface area and porosity analyzer. Before analysis, the samples were allowed to dry under vacuum and degas at 50 °C for 8 h under vacuum (10^{-5} bar).

Supporting Information

Supporting Information, including additional figures and movies, is available from the Wiley Online Library or from the author.

Acknowledgements

This work was supported by the funds from the National Basic Research Program of China (973 Program, 2012CB812500, 2012CB932500), National Natural Science Foundation of China (21004025 and 91127046), Chinese Ministry with NCET-10-0398, and Fundamental Research Funds for the Central Universities (HUST: 2010MS081). We also thank the HUST Analytical and Testing Center for allowing us to use its facilities.

Received: November 28, 2011
Revised: December 2, 2011
Published online: February 2, 2012

[1] R. S. Kane, *Angew. Chem. Int. Ed.* **2008**, *47*, 1368.
[2] Z. H. Nie, S. Q. Xu, M. Seo, P. C. Lewis, E. Kumacheva, *J. Am. Chem. Soc.* **2005**, *127*, 8058.
[3] H. Yabu, T. Higuchi, M. Shimomura, *Adv. Mater.* **2005**, *17*, 2062.

[4] S. J. Jeon, G. R. Yi, S. M. Yang, *Adv. Mater.* **2008**, *20*, 4103.
[5] L. Wang, Y. Yamauchi, *Chem. Mater.* **2009**, *21*, 3562.
[6] J. A. Champion, S. Mitragotri, *Proc. Natl. Acad. Sci. USA.* **2006**, *103*, 4930.
[7] T. Deng, J. R. Cournoyer, J. H. Schermerhorn, J. Balch, Y. Du, M. L. Blohm, *J. Am. Chem. Soc.* **2008**, *130*, 14396.
[8] L. B. Koh, I. Rodriguez, S. S. Venkatraman, *Biomaterials* **2010**, *31*, 1533.
[9] P. E. Scopelliti, A. Borgonovo, M. Indrieri, L. Giorgetti, G. Bongiorno, R. Carbone, A. Podesta, P. Milani, *Plos One* **2010**, *5*, e11862.
[10] T. Tanaka, Y. Komatsu, T. Fujibayashi, H. Minami, M. Okubo, *Langmuir* **2010**, *26*, 3848.
[11] S. Q. Xu, Z. H. Nie, M. Seo, P. Lewis, E. Kumacheva, H. A. Stone, P. Garstecki, D. B. Weibel, I. Gitlin, G. M. Whitesides, *Angew. Chem. Int. Ed.* **2005**, *44*, 724.
[12] A. S. Utada, E. Lorenceau, D. R. Link, P. D. Kaplan, H. A. Stone, D. A. Weitz, *Science* **2005**, *308*, 537.
[13] H. F. Huang, H. R. Liu, *J. Polym. Sci. Polym. Chem.* **2010**, *48*, 5198.
[14] T. Zhao, D. Qiu, *Langmuir* **2011**, *27*, 12771.
[15] J. T. Zhu, R. C. Hayward, *Angew. Chem. Int. Ed.* **2008**, *47*, 2113.
[16] J. T. Zhu, N. Ferrer, R. C. Hayward, *Soft Matter* **2009**, *5*, 2471.
[17] E. Pisani, C. Ringard, V. Nicolas, E. Raphaël, V. Rosilio, L. Moine, E. Fattal, N. Tsapis, *Soft Matter* **2009**, *5*, 3054.
[18] J. T. Zhu, R. C. Hayward, *J. Am. Chem. Soc.* **2008**, *130*, 7496.
[19] J. C. López-Montilla, P. E. Herrera-Morales, S. Pandey, D. O. Shah, *J. Disper. Sci. Technol.* **2002**, *23*, 219.
[20] K. Chang, C. W. Macosko, D. C. Morse, *Macromolecules* **2007**, *40*, 3819.
[21] J. B. Jiao, E. J. Kramer, S. de Vos, M. Möller, C. Koning, *Macromolecules* **1999**, *32*, 6261.
[22] R. Granek, R. C. Ball, M. E. Cates, *J. Phys. II* **1993**, *3*, 829.
[23] G. Ruan, J. O. Winter, *Nano Lett.* **2011**, *11*, 941.
[24] K. R. Shull, A. J. Kellock, V. R. Deline, S. A. Macdonald, *J. Chem. Phys.* **1992**, *97*, 2095.
[25] J. G. Hu, R. Granek, *J. Phys. II* **1996**, *6*, 999.
[26] J. T. Zhu, R. C. Hayward, *Macromolecules* **2008**, *41*, 7794.
[27] J. T. Zhu, R. C. Hayward, *J. Colloid Interf. Sci.*2012, *365*, 275.
[28] B. J. Kim, H. M. Kang, K. Char, K. Katsov, G. H. Fredrickson, E. J. Kramer, *Macromolecules* **2005**, *38*, 6106.
[29] M. S. El-Aasser, C. D. Lack, J. W. Vanderhoff, F. M. Fowkes, *Colloids Surf.* **1988**, *29*, 103.
[30] D. Walsh, B. Lebeau, S. Mann, *Adv. Mater.* **1999**, *11*, 324.
[31] J. F. Foster, R. M. Hixon, *J. Am. Chem. Soc.* **1944**, *66*, 557.
[32] F. Xia, L. Jiang, *Adv. Mater.* **2008**, *20*, 2842.
[33] P. Roach, N. J. Shirtcliffe, M. I. Newton, *Soft Matter* **2008**, *4*, 224.
[34] W. W. Yu, X. G. Peng, *Angew. Chem. Int. Ed.* **2002**, *41*, 2368.
[35] J. Park, K. J. An, Y. S. Hwang, J. G. Park, H. J. Noh, J. Y. Kim, J. H. Park, N. M. Hwang, T. Hyeon, *Nat. Mater.* **2004**, *3*, 891.